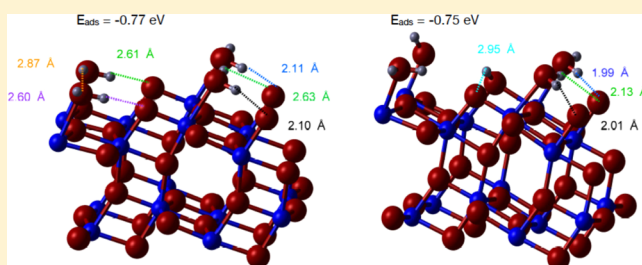


First-Principles Study of the Water Adsorption on Anatase(101) as a Function of the Coverage

Ruth Martinez-Casado,^{*,†,‡,§,||} Giuseppe Mallia,^{||} Nicholas M. Harrison,^{||} and Rubén Pérez^{*,§,⊥,||}[†]Dipartimento Chim, IFM, Univ. Turin, I-10125 Turin, Italy[‡]Centro Ricerche Fiat SCpA, Strada Torino 50, 10043 Orbassano (TO), Italy[§]Departamento de Física Teórica de la Materia Condensada, Universidad Autónoma de Madrid, E-28049 Madrid, Spain^{||}Department of Chemistry, Imperial College London, South Kensington, SW7 2AZ London, U.K.[⊥]Condensed Matter Physics Center (IFIMAC), Universidad Autónoma de Madrid, 28049 Madrid, Spain

ABSTRACT: An understanding of the interaction of water with the anatase(101) surface is crucial for developing strategies to improve the efficiency of the photocatalytic reaction involved in solar water splitting. Despite a number of previous investigations, it is still not clear if water preferentially adsorbs in its molecular or dissociated form on anatase(101). With the aim of shedding some light on this controversial issue, we report the results of periodic screened-exchange density functional theory calculations of the dissociative, molecular, and mixed adsorption modes on the anatase(101) surface at various coverages. Our calculations support the suggestion that surface-adsorbed OH groups are present, which has been made on the basis of recently measured X-ray photoelectron spectroscopy, temperature-programmed desorption, and scanning tunneling microscopy data. It is also shown that the relative stability of water adsorption on anatase(101), at different configurations, can be understood in terms of a simple model based on the number and nature of the hydrogen bonds formed as well as the adsorbate-induced atomic displacements in the surface layers. These general conclusions are found to be insensitive to the specific choice of approximation for electronic exchange and correlation within the density functional theory. The simple model of water–anatase interactions presented here may be of wider validity in determining the geometry of water–oxide interfaces.



1. INTRODUCTION

TiO₂, as a wide-band-gap semiconductor, has many applications, including as a heterogeneous catalyst,¹ as the transport medium in dye-sensitized solar cells,² and as the catalyst in photoelectrochemical water splitting for the carbon-free production of hydrogen.^{3,4} An understanding of water chemistry on TiO₂ is crucial to facilitate the design of more efficient systems. Water can adsorb on TiO₂ surfaces molecularly or dissociatively. Molecular adsorption (in its most energetically favorable configuration) involves the direct interaction of the oxygen atom of the molecule with the 5-fold-coordinated titanium, Ti_{5c}, of the surface. In the dissociative adsorption mode, a hydrogen atom is transferred from the molecule to a nearby under-coordinated surface oxygen ion. Two surface hydroxyls are thus formed: the hydroxyl bonded to the surface Ti_{5c}, which is generally called terminal hydroxyl OH_{th}, and that resulting from the detached hydrogen and nearby oxygen ion, called the bridging hydroxyl OH_{bh}.

Rutile is the most stable bulk phase of titania; however, anatase nanoparticles are the most active photocatalyst.^{5–7} The (101) surface is the most stable anatase surface and represents a significant portion of the exposed surface area in nanostructures.^{8–10} Despite significant research effort in this

area, there is still controversy over the nature of the first water monolayer (ML) on the anatase(101) surface and, in particular, whether there is molecular or dissociative adsorption. This is also an open problem for the (110) surface of rutile.^{7,11} Until a few years ago, X-ray photoelectron spectroscopy (XPS),¹² temperature-programmed desorption,¹² and scanning tunneling microscope (STM)¹³ experiments seemed to agree with density functional theory (DFT) calculations^{14–16} that only molecular adsorption occurs on the pristine anatase(101) surface. Two recent high-resolution XPS¹⁷ and X-ray diffraction¹⁸ studies, however, reported the presence of OH groups at the surface and challenged the accepted model of the interface. Subsequent DFT^{19,20} and force field²¹ studies support this result, predicting mixed molecular and dissociative adsorption on anatase(101) for coverages from half to one monolayer. In recent calculations, the detailed energetics of adsorption has been computed using hybrid-exchange density functional theory, PBE0, but without an analysis of the structure at the full monolayer coverage that

Received: May 28, 2018

Revised: August 12, 2018

Published: August 13, 2018

Table 1. All-Electron Basis Set Hierarchy for Ti, O, and H

	Ti	O	H
BS1	8-6411d(1) (1s;4sp;1d)	8-611(1s;3sp)	3-1p(1) (2s;1p)
BS2	8-6411d(11) (1s;4sp;2d)	8-611	3-1p(1)
BS3	8-6411d(11)	8-611(d1) (1s;3sp;1d)	3-1p(1)

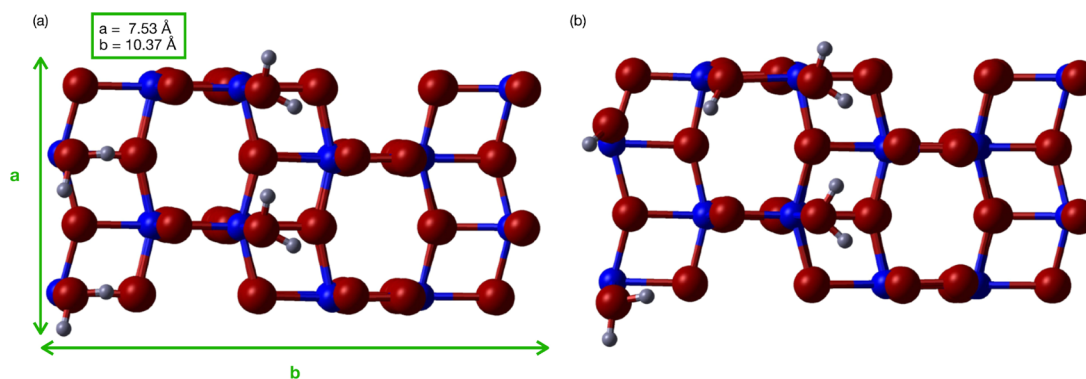


Figure 1. (Color online) Top view of the optimized structures resulting from the adsorption of water on anatase(101) at full monolayer coverage and for the cases: (a) molecular adsorption by using the HSE functional and (b) mixed adsorption by using the HSE functional. Large (red), medium (blue), and small (gray) spheres correspond to oxygen, titanium, and hydrogen, respectively.

is observed or a discussion of the number and nature of the hydrogen bonds present at the interface.¹⁹

It is now well established that consideration of intermolecular interactions is essential for an understanding of the water–oxide interface structure.^{22,23}

An accurate quantum treatment of these hydrogen bonds is mandatory for a proper description of the interface structure and properties.^{24,25} The purpose of the present work is to shed some light on the nature of the water–water and water–anatase(101) interactions that determine the interfacial structure. To achieve this, calculations are performed as a function of the coverage (defined as the ratio between the number of adsorbed H₂O molecules and the number of surface Ti_{5c} sites).

The adopted method is DFT using the screened hybrid-exchange functional Heyd–Scuseria–Ernzerhof (HSE);²⁶ we also present results obtained with the gradient-corrected Perdew–Burke–Ernzerhof (PBE) functional to determine the sensitivity of the conclusions to the approximate treatment of electronic exchange and correlation. The HSE functional has the advantage that, in general, it describes surface adsorption energetics and structures somewhat better than the PBE functional, partially corrects for electronic self-interaction and so yields qualitatively correct fundamental band gaps in wide-band-gap transition metal oxides, and retains a reasonable description of semiconductors and metals.^{27,28} Compared to other hybrid functionals, like PBE0, HSE performs much better in predicting the properties of many solids.²⁹ Furthermore, two very recent works^{30,31} have shown that PBE0 tends to overestimate the band gaps, while HSE is more accurate for typical semiconductors.

The results and discussion presented here lead to the idea that water adsorption on anatase(101) can be described by a simple model that supports the suggestion that OH groups are present at the surface. This model emphasizes the importance of the number and nature of the adsorbate–adsorbate and adsorbate–surface hydrogen bonds for determining the structure of the interface.

2. COMPUTATIONAL DETAILS

All calculations have been performed using the CRYSTAL14 software package,³² based on the expansion of the crystalline orbitals as a linear combination of a local basis set (BS) consisting of atom-centered Gaussian orbitals with s, p, or d symmetry.

The choice of the BS is the main numerical approximation in these calculations; to approach the BS limit, a hierarchy of all-electron basis sets, labeled as BS1, BS2, and BS3 (see Table 1), has been selected for O, Ti. The most complete basis set (BS3) has been used for the calculations.

The anatase structure belongs to the *I4/amd* tetragonal space group, and the unit cell is defined by the lattice vectors *a* and *c* and the oxygen internal coordinate *u*. The primitive cell contains two atoms in the asymmetric unit: a Ti ion at (0,0,0) and an O ion at (0,0,*u*), in fractional coordinates. Each Ti is octahedrally coordinated to six O ions. The TiO₆ octahedron is distorted, with the length of the two apical (Ti–O)_{ap} bonds slightly longer than the four equatorial, (Ti–O)_{eq} bonds. The anatase TiO₆ octahedron shares four edges in adjacent pairs.

The surface is simulated by using a slab, which is periodic in two dimensions (2D) but finite in the third, for which the boundary condition is that the wave function decays to zero at infinite distance from the surface. The slab is cut from the bulk crystal fully optimized with respect to lattice parameters and atomic coordinates. The slab consists of four TiO₂ trilayers with the in-plane periodicity given by a 1 × 2 supercell of the conventional surface cell. The surface unit cell dimensions are therefore 10.48 × 7.60 Å for PBE and 10.37 × 7.53 Å for HSE (see Figure 1).

Integration over reciprocal space was carried out on a symmetrized Monkhorst–Pack³³ with shrinking factor 4 for the 2D slab cell (and the shrinking factor was kept consistent for supercells).

Matrix elements of the exchange and correlation potentials and the energy functional are integrated numerically on an atom-centered grid of points. The integration over radial and angular coordinates is performed using Gauss–Legendre and Lebedev schemes, respectively. A pruned grid consisting of 99

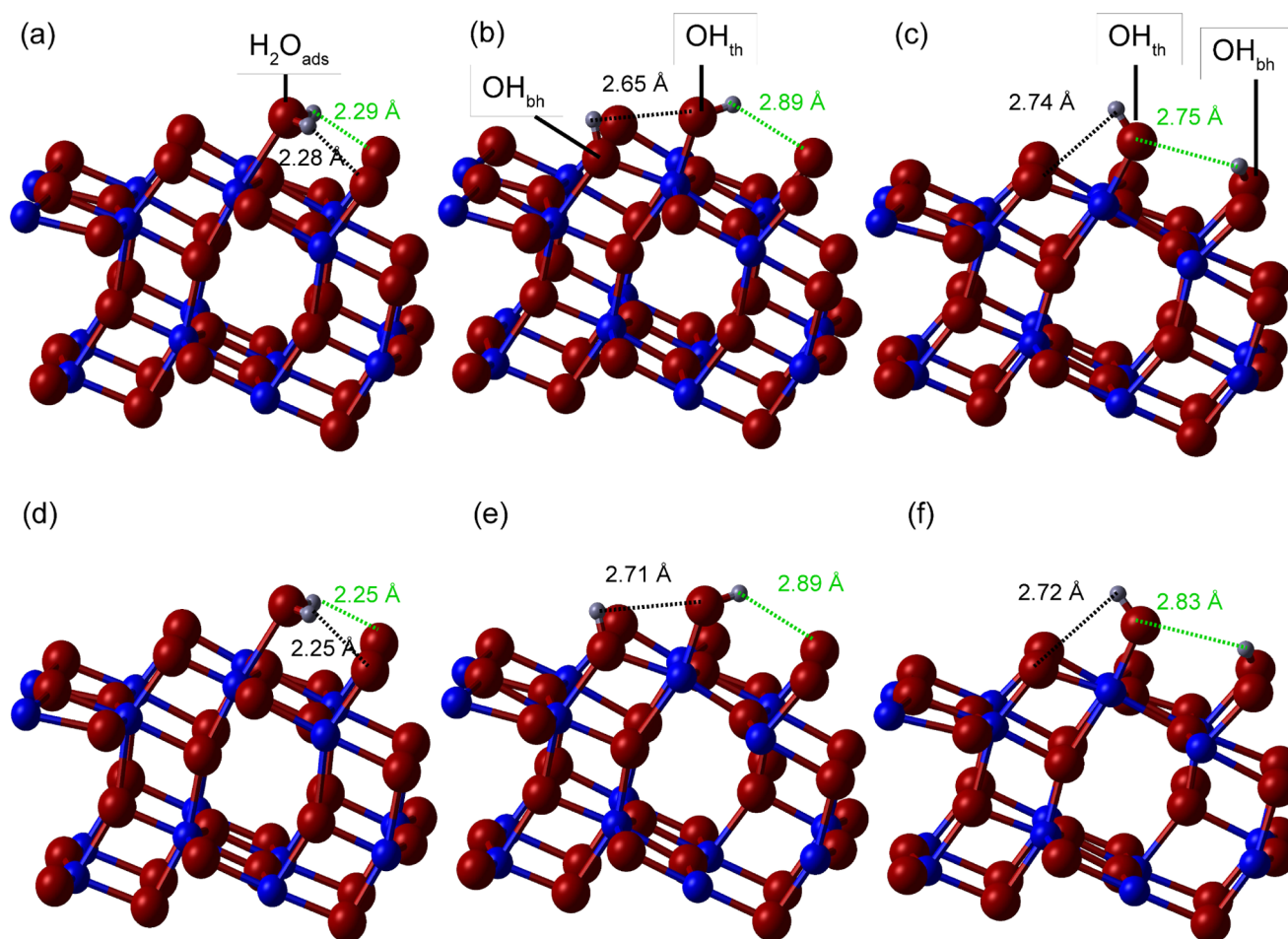


Figure 2. (Color online) Optimized structures and hydrogen bonds resulting from the adsorption of water on anatase(101) at the dilute limit for (a) HSE molecular, (b) HSE intramolecular dissociative, (c) HSE intermolecular dissociative, (d) PBE molecular, (e) PBE intramolecular dissociative, and (f) PBE intermolecular dissociative cases. O2–H distance is shown with dashed lines.

Table 2. Adsorption Energies as a Function of the Coverage for the HSE and PBE Functionals^a

Coverage (Θ)	Method	E_{ads} (eV)			
		Mol	Dis(Intra)	Dis(Inter)	Diff(Dis(Inter)-Mol)
0.25	LCAO-PBE	-0.71	-0.38	-0.34	0.37
0.25	LCAO-HSE	-0.84	-0.54	-0.49	0.35
0.25	PW-PBE ¹⁹	-0.69	-0.42	-0.37	0.32
Coverage (Θ)	Method	Mol	Mixed(Intra)	Mixed(Inter)	Diff(Mixed(Inter)-Mol)
0.5	LCAO-PBE	-0.70		-0.63	0.07
0.5	LCAO-HSE	-0.81		-0.75	0.06
1.0	LCAO-PBE	-0.68		-0.65	0.02
1.0	LCAO-HSE	-0.77		-0.75	0.02
1.0	PW-PBE ¹⁹	-0.64		-0.58	0.06

^aPrevious plane-wave (PW) results with the PBE functional have been added for comparison.

radial points and five subintervals with (146, 302, 590, 1454, 590) angular points has been used for all calculations (the XXLGRID option implemented in CRYSTAL14³²). This grid converges the integrated charge density to an accuracy of about 10^{-6} electrons per unit cell. The Coulomb and exchange series are summed directly and truncated using overlap criteria with thresholds of [7,7,7,7,14].³⁴

The self-consistent field iterations were considered to be converged when the change in energy was less than 10^{-7} Hartree per cell. Structural optimization of internal coordinates was performed using the Broyden–Fletcher–Goldfarb–

Shanno scheme. Convergence was determined from the root-mean-square (rms) and the absolute value of the largest component of the forces. The thresholds for the maximum and the rms forces (the maximum and the rms atomic displacements) were set to 0.02 and 0.01 eV/Å (0.0009 and 0.0006 Å, respectively). Geometry optimization was terminated when all four conditions were satisfied simultaneously.

3. RESULTS AND DISCUSSION

3.1. Dilute Limit. An initial model of isolated molecular adsorption is generated by placing a molecule above one of the

four Ti_{5c} sites of the 2×1 surface supercell discussed above (Figure 2a,d). This corresponds to a coverage of $\Theta = 0.25$ ML with the minimum intermolecular spacing being 10.5 \AA at which distance intermolecular interactions may be considered to be negligible.¹⁹ Isolated dissociative adsorption is modeled by placing an OH_{th} group above the Ti_{5c} site and a proton at a surface 2-fold coordinate O ion (O_{2c}), thereby generating a bridging hydroxyl group, OH_{bh} . There are two possible configurations based on the hydrogen bond (H-bond) distance: intrapair [interpair] when the H-bond distance between the O atom of the OH_{th} and the detached H of the OH_{bh} is shorter [longer] than the distance between the H of the OH_{th} and its acceptor, the lattice O (Figure 2b,e) and interpair (Figure 2b,e[2c,f]). Both molecular and dissociative adsorption modes are found to be locally stable during geometry optimization (see Table 2).

Our results with both PBE and HSE show that molecular adsorption is clearly preferred by ~ 0.3 eV on anatase at low coverage, in agreement with previous calculations¹⁹ and recent experimental results in anatase.³⁵ Interestingly, this behavior is completely different from the one found in rutile, where the molecular and dissociative adsorption states are very close in energy in the dilute limit.^{7,11}

A simple model based on the analysis of the hydrogen bonding can be used to rationalize the computed adsorption energies. The hydrogen bond in water involves a hydrogen (H), the oxygen (O1) to which it is covalently bound, and a second hydrogen bond acceptor oxygen ion (O2). There are many classifications for the hydrogen bond in the literature; the one presented in Table 3 is the most commonly used and

Table 3. Classification of Hydrogen Bonds

	strong	medium	weak
bond energy (eV)	0.17–1.73	0.17–0.61	0.0–0.17
type	covalent	mostly electrostatic	electrostatic
distance (O1–O2) (Å)	2.2–2.5	2.5–3.2	3.2–4.0
distance (H–O2) (Å)	1.2–1.5	1.5–2.2	2.2–3.2
bond angle (°)	175–180	130–180	90–150

relates the strength of the bond to the O1–O2 and H–O2 distances.³⁶ An alternative method to assess the strength of hydrogen bonds has been recently presented, based on the proton-transfer coordinate ν , which is defined as $\nu = \text{distance}(\text{H–O1}) - \text{distance}(\text{H–O2})$; hydrogen bonds are not formed for $\nu \geq -1.25 \text{ \AA}$.²⁴ In the current context, both classification methods yield the same conclusion that for a $\text{distance}(\text{H–O2}) \geq 2.3 \text{ \AA}$, only weak hydrogen bonds are formed. The optimized structures computed in the HSE and PBE approximations are displayed in Figure 2, together with the computed H–O2 distances. Molecular adsorption yields two medium-strength hydrogen bonds in both approximations, while the dissociated water yields two weak bonds for both the intrapair and interpair configurations.

The presence of a medium-strength hydrogen bond implies a contribution to the binding energy of around 0.17 eV (see Table 3), which is consistent with the fact that the computed energy of molecular adsorption (with two medium-strength hydrogen bonds) is found to be more favorable by 0.30 eV than dissociative adsorption. This simple model is consistent with the calculated adsorption energies of each configuration in Table 2.

To check the possible effect of dispersion terms not included in the used functionals, we performed a geometry optimization of atomic coordinates for the molecular and intramolecular adsorptions by using the PBE-D3³⁷ approximation. The structures obtained with this method were very similar to the ones showed in Figure 2 for PBE only. In particular, the Ti–O distances predicted by both approaches differ in less than 0.01 Å. Regarding the adsorption energy, the new values including the van der Waals contribution with PBE-D3 are -0.60 and -0.93 eV for the intramolecular and molecular adsorption, respectively. Comparing with the results in Table 2 for PBE (-0.38 and -0.71 eV), we confirm that there is no change in the energy difference (-0.33 eV) between these two configurations. Taking into account these results, we do not expect a significant change in the main conclusions of this work by adding the van der Waals contribution.

To understand how the adsorption structure affects the photochemistry of the surface, the projections of the density of states (DOS) on the eight outermost Ti_{5c} and O_{2c} atoms plus water are presented in Figure 3 for the HSE functional. In the DOS of the anatase(101) surface (see Figure 3a), the valence band—below -5 eV—displays predominantly O 2p character, with some hybridization with Ti 3d orbitals; the conduction band—above 0 eV—is derived mainly from Ti 3d atomic orbitals with some hybridization with O 2p orbitals.^{10,38,39} No significant changes can be seen when a water molecule is molecularly adsorbed on the surface (Figure 3b). On the other hand, the dissociatively adsorbed molecules display significant hybridization of the molecular O 2p states with those of the surface (Figure 3c,d). The results presented in this section are in agreement with previous DFT works^{14,15,19} and generally support a model in which molecular adsorption dominates at the dilute limit.

3.2. Half Monolayer Coverage. In the molecular adsorption at half monolayer coverage ($\Theta = 0.5$ ML), two water molecules are placed above two of the four Ti_{5c} sites of the (101) surface. There is a significant change in the optimized structure compared to the dilute case, as shown in Figure 4, in calculations with both HSE and PBE approximations. Water is a polar molecule with a partial negative charge at the oxygen end, while hydrogen atoms are partially positively charged. The hydrogen atoms of contiguous water molecules tend to repel each other, favoring the formation of a hydrogen bond with the oxygen atom of the neighboring water molecule. This behavior, where three weak hydrogen bonds are formed, is reproduced by both considered functionals.

Concerning the mixed molecular-dissociated adsorption, we present here the most energetically favorable configuration according to our calculations, which is consistent with that previously reported.^{17,19,40} In this configuration, shown in Figure 4b,d, the OH_{th} group (at the Ti_{5c} site) and the OH_{bh} group form a hydrogen bond, ending up in three weak hydrogen bonds. The undissociated molecule and OH_{th} show hydrogen bonds with a neighboring O_{2c} while the H in OH_{bh} is linked to the O in OH_{th} , and the H in OH_{th} is linked in turn to another neighboring O_{2c} . As a consequence, the same number of weak bonds is formed as in molecular adsorption. The optimized structures for the mixed adsorption are very similar for both functionals (Figure 4).

We have considered the detached hydrogen atom to form the OH_{bh} with the two possible O_{2c} sites allowed by our

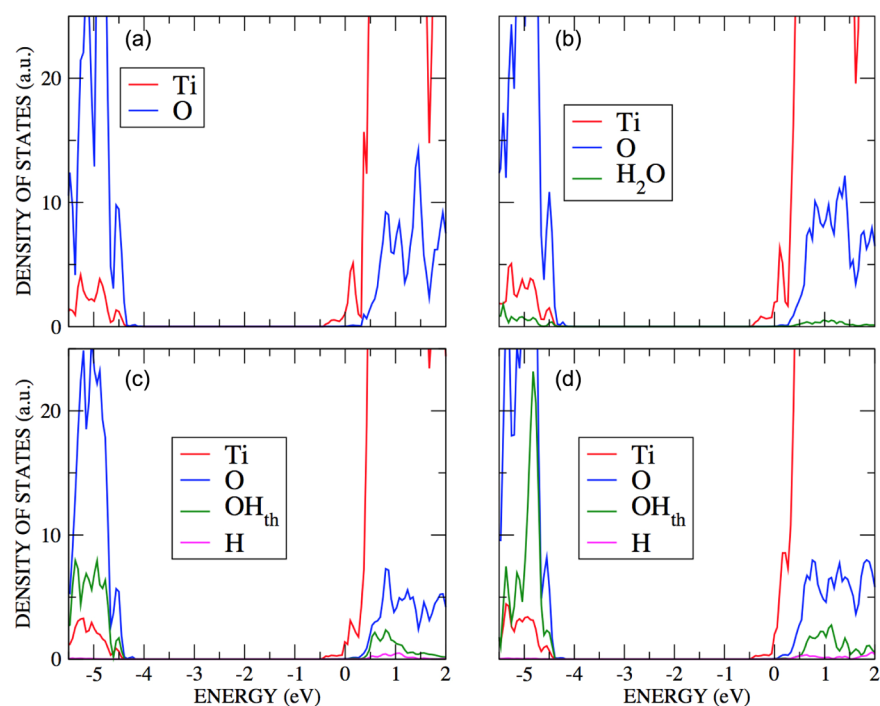


Figure 3. (Color online) DOS for anatase(101) at the dilute limit projected on the eight outermost Ti_{5c} and O_{2c} atoms plus water, when using the HSE functional, for the following cases: (a) clean surface, (b) molecular adsorption of water, (c) intramolecular dissociative adsorption of water, and (d) intermolecular dissociative adsorption of water.

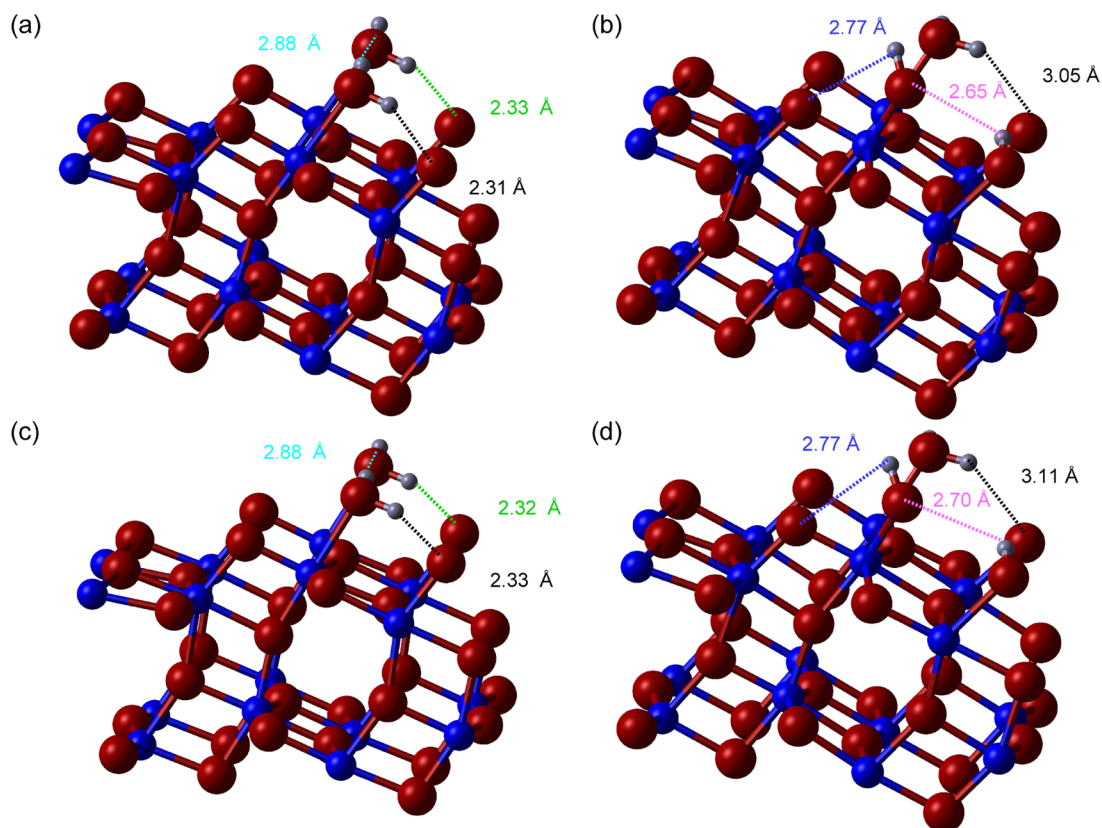


Figure 4. (Color online) Optimized structures and hydrogen bonds resulting from the adsorption of water on anatase(101) at half monolayer coverage and the cases (a) HSE molecular, (b) HSE mixed, (c) PBE molecular, and (d) PBE mixed. $\text{O}_2\text{--H}$ distance is shown with dashed lines.

supercell, with the one presented in Figure 4 being lower in energy.

The DOS projected on the eight outermost Ti_{5c} and O_{2c} atoms plus water computed in the HSE approximation is presented in Figure 5.

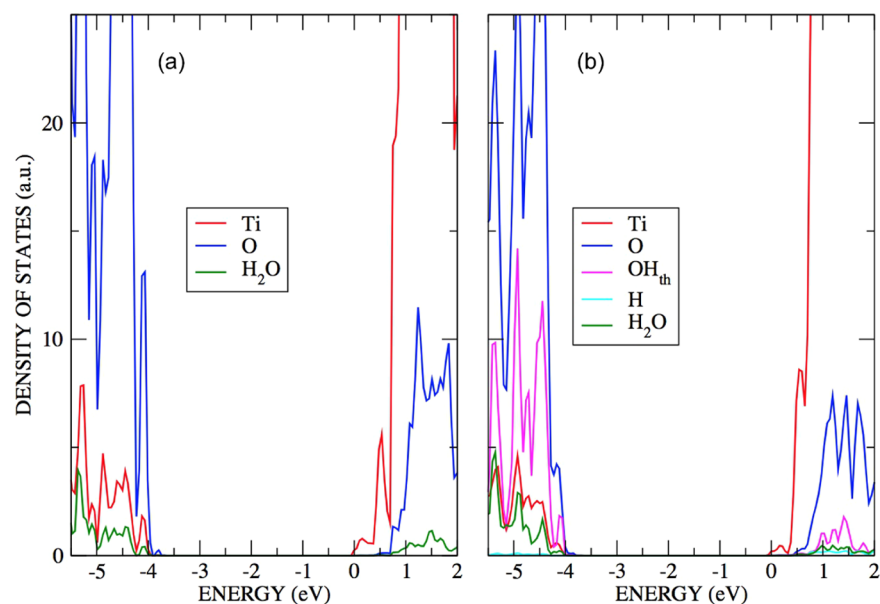


Figure 5. (Color online) DOS for anatase(101) at half monolayer coverage projected on the eight outermost Ti_{5c} and O_{2c} atoms plus water and using the HSE functional for the cases (a) molecular adsorption of water and (b) mixed adsorption of water.

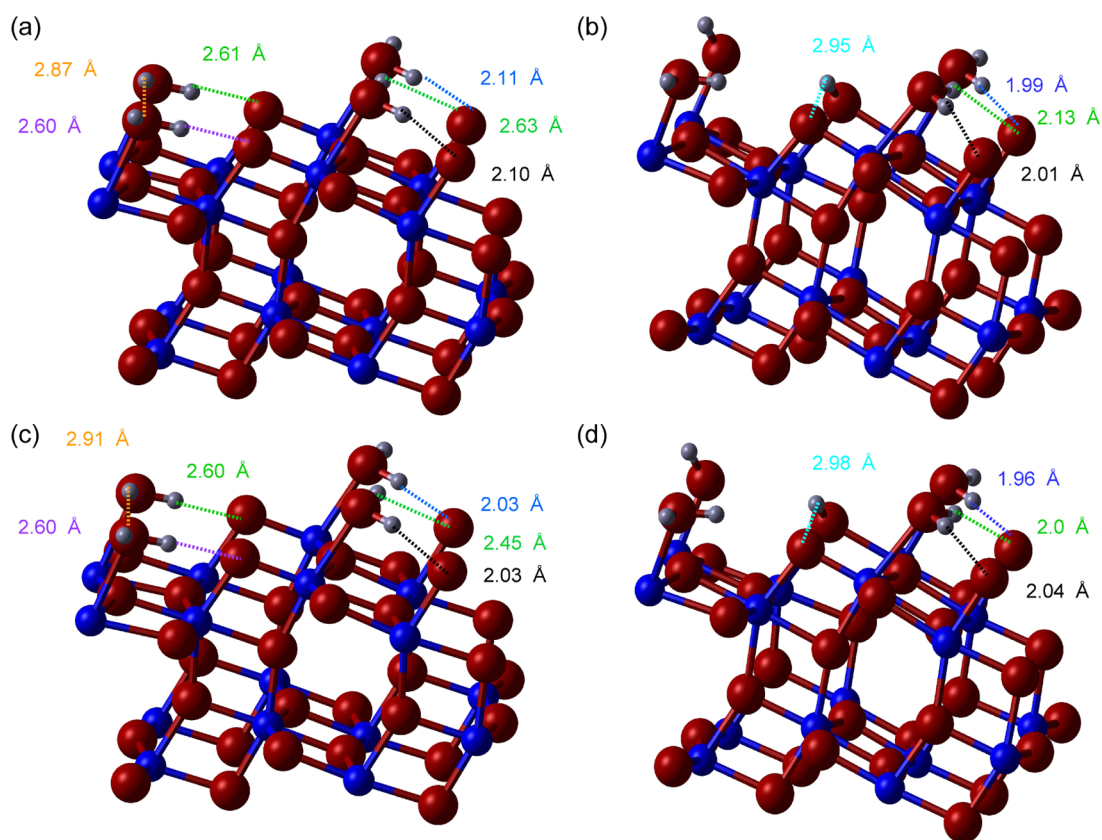


Figure 6. (Color online) Optimized structures and hydrogen bonds resulting from the adsorption of water on anatase(101) at full monolayer coverage and the cases (a) HSE molecular, (b) HSE mixed, (c) PBE molecular, and (d) PBE mixed. $\text{O}_2\text{--H}$ distance is shown with dashed lines.

In this mixed adsorption configuration, the O states from OH_{th} are strongly hybridized with the O states of the surface valence band—below -4 eV.

An analysis of the adsorption energies in Table 2 leads us to the conclusion that molecular and mixed adsorption modes have a very similar stability at half monolayer coverage; this is consistent with the number and type of bonds present. The

DFT energy therefore suggests that the mixed adsorption is stable, something that is confirmed by the simple bonding model presented here.

This result supports the conclusion that OH groups are present at the anatase(101) surface recently obtained from analysis of XPS data.¹⁷

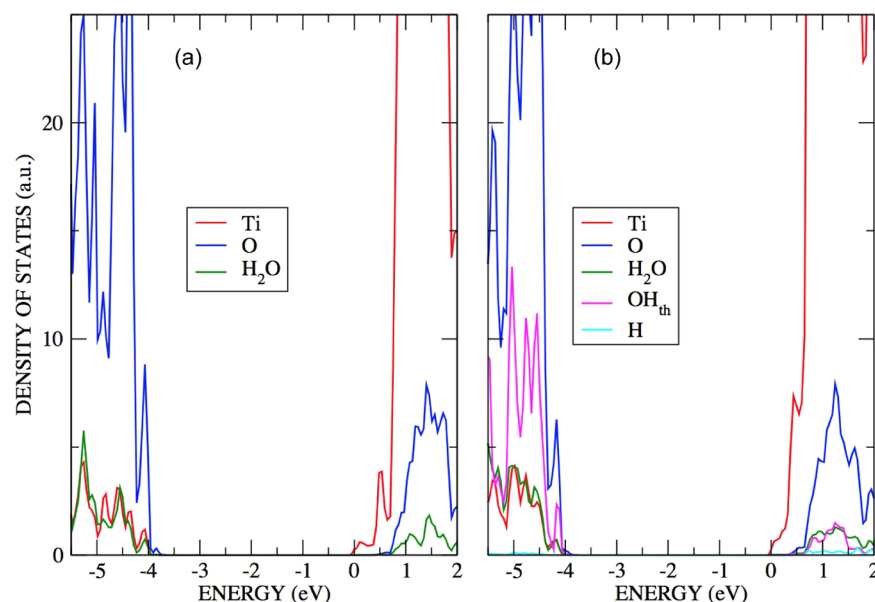


Figure 7. (Color online) DOS for anatase(101) at full monolayer coverage projected on the eight outermost Ti_{5c} and O_{2c} atoms plus water and using the HSE functional for the cases (a) molecular adsorption of water and (b) mixed adsorption of water.

3.3. Full Monolayer Coverage. Based on XPS measurements at low temperature (LT), it has been suggested that at full monolayer coverage, around 25% of the water molecules are dissociated.¹⁷ We have explored this possibility by investigating a number of water–oxide interface configurations, one consisting of only molecular adsorption and several in which 25% of the molecules are dissociated (Figure 6a,c). The relaxed geometries of the molecular and lowest energy mixed configurations, among those consistent with the adopted 2D periodicity, found in the HSE and PBE approximations are displayed in Figure 6.

For molecular adsorption, the water molecules form two medium and four weak hydrogen bonds. In the mixed adsorption, two of the undissociated molecules form three medium hydrogen bonds, while the OH_{th} group has a weak hydrogen bond to an O_{2c} . This overall bonding is insensitive to the choice of density functional.

The adsorption energies presented in Table 2 suggest that at full coverage, as at half coverage, molecular and mixed adsorption modes have very similar energies (within 0.02 eV). This is consistent with the model suggested on the basis of XPS experiments.¹⁷ It is notable that a similar conclusion has been reached on the basis of STM data for water adsorbed at the rutile (110) surface.¹¹ The remarkably small change in the energy when one water molecule undergoes dissociation can be understood in terms of the H-bonding model. The loss of two of the three weak hydrogen bonds present in the molecular adsorption configuration is compensated by the formation of a medium-strength H-bond between a remaining undissociated water molecule and a neighboring O_{2c} .

The DOS for configurations at 1 ML coverage is presented in Figure 7; there are no significant differences with respect to the 0.5 ML coverage. In both projected DOS plots (Figures 5 and 7), the oxygen states of OH_{th} are strongly hybridized with the O states of anatase(101) at the top the valence band. This behavior is different with respect to other oxides such as SnO_2 , where water molecules dissociate but no hybridization of the resulting hydroxyls with the oxide states has been found.⁴¹

Recent X-ray diffraction experiments by Nadeem et al.¹⁸ have explored the structure of the water–oxide interface under very different conditions regarding the temperature and thickness of the water layer compared to the experiments by Sandell et al.¹⁷ that we have considered in our work. While ref 17 claims that 25% of water molecules are dissociated for 1 ML coverage at low temperatures (LT, 220 K), the new experiments¹⁸ show that 75% is dissociated for a thick layer of water (at least 8 MLs) at room temperature (RT, around 300 K). Figure 4a in ref 17 already shows this temperature dependence, suggesting that 25% of the molecules will be dissociated at 220 K and 75% of them at 300 K.

Both experiments agree in predicting that a mixed interface, with both molecular and dissociated water, is the most stable configuration. Our results prove that the increase in the water coverage favors the mixed interface and support the fraction of 25% dissociated molecules for the 1 ML case at LT found in ref 17. On the other hand, our calculations for the Ti–O (from $\text{H}_2\text{O}_{\text{ads}}$) and Ti– OH_{th} bond lengths in the mixed interface are in excellent agreement with the new X-ray diffraction results.¹⁸ We attribute the discrepancy in the fraction of dissociated water molecules between the two experimental studies to the very different experimental conditions: low coverage and LT (ref 17) vs a thick water layer at RT (ref 18).

4. CONCLUSIONS

In this study, the interaction of water with anatase(101) has been explored, as a function of the coverage, by analyzing the geometrical and electronic properties. A detailed characterization of this system could help in the prediction of the structure and properties of other water–oxide interfaces. The model presented here is characterized by an interplay among chemisorption, hydrogen bonding, and atomic displacements at the surface. Molecular, dissociative, and mixed adsorption modes have been investigated at various coverages showing the mixed one to be more favorable as coverage increases. The projected density of states of the surface in contact with a mixture of adsorbed water molecules and adsorbed hydroxyls clarifies the nature of the chemical bonds involved. Adsorbed

water states on anatase(101) hybridize strongly with the O 2p states of the surface. This hybridization is not shown in other oxides such as SnO₂, although water molecule appears to be dissociated in this surface.⁴¹

An analysis of the adsorption energies leads us to the conclusion that molecular and mixed dissociated adsorptions have a very similar stability at half and full monolayer coverages, which is confirmed by the simple bonding model presented here. This result is consistent with the finding of OH groups at the anatase(101) surface recently reported by XPS.^{17,18} There is, however, a discrepancy between the percentage of dissociated water between these two experiments that we attribute to the very different conditions regarding the temperature and thickness of the water layer. Our total energy calculations, suitable for the LT case, agree with the earlier experiments by Sandell et al.,¹⁷ where 25% of water molecules are dissociated for 1 ML coverage. In the case of the recent RT experiments, considering a thick water layer, the theoretical evaluation of the relative stability of different phases requires the complex calculation of free energies. We expect that our paper, in combination with the recent experimental results, will stimulate work in this direction.

Given that obtaining a reliable and clean water–anatase interface is far from trivial from an experimental point of view, theoretical results as the ones reported here are a valuable contribution to the characterization of the water–anatase interaction, and we hope that they will motivate further experimental and theoretical work to achieve a complete understanding of this technologically relevant interface.

AUTHOR INFORMATION

Corresponding Authors

*E-mail: ruthmcasado@gmail.com (R.M.-C.).

*E-mail: ruben.perez@uam.es (R.P.).

ORCID

Ruth Martinez-Casado: 0000-0003-0038-8669

Rubén Pérez: 0000-0001-5896-541X

Notes

The authors declare no competing financial interest.

ACKNOWLEDGMENTS

Financial support from the Spanish MINECO under grants MAT2014-54484-P, MAT2017-83273-R, and the Juan de la Cierva Program is gratefully acknowledged. Computer time was provided by the Spanish Supercomputing Network (RES, Spain) at the Magerit Supercomputer (Madrid, Spain). This work made use of the high-performance computing facilities of Imperial College London and via our membership of the U.K. HPC Materials Chemistry Consortium, which is funded by EPSRC (EP/L000202).

REFERENCES

- (1) Haruta, M.; Yamada, N.; Kobayashi, T.; Iijima, S. Gold catalysts prepared by coprecipitation for low-temperature oxidation of hydrogen and of carbon monoxide. *J. Catal.* **1989**, *115*, 301–309.
- (2) Grätzel, M. Photoelectrochemical cells. *Nature* **2001**, *414*, 338–344.
- (3) Fujishima, A.; Honda, K. Electrochemical Photolysis of Water at a Semiconductor Electrode. *Nature* **1972**, *238*, 37–38.
- (4) Listorti, A.; Durrant, J.; Barber, J. Structure and dynamics of liquid water on rutile TiO₂ (110). *Nat. Mater.* **2009**, *8*, 929–930.

- (5) Crossland, E. J. W. Mesoporous TiO₂ single crystals delivering enhanced mobility and optoelectronic device performance. *Nature* **2013**, *495*, 215–219.

- (6) Murdoch, M.; Waterhouse, G. I. N.; Nadeem, M. A.; Metson, J. B.; Keane, M. A.; Howe, R. F.; Llorca, J.; Idriss, H. The effect of gold loading and particle size on photocatalytic hydrogen production from ethanol over Au/TiO₂ nanoparticles. *Nat. Chem.* **2011**, *3*, 489–492.

- (7) Balajka, J.; Aschauer, U.; Mertens, S.; Selloni, A.; Schmid, A.; Diebold, U. Surface Structure of TiO₂ Rutile (011) Exposed to Liquid Water. *J. Phys. Chem. C* **2017**, *121*, 26424–26431.

- (8) Labat, F.; Baranek, P.; Adamo, C. Structural and Electronic Properties of Selected Rutile and Anatase TiO₂ Surfaces: An ab Initio investigation. *J. Chem. Theory Comput.* **2008**, *4*, 341–352.

- (9) Lazzeri, M.; Vittadini, A.; Selloni, A. Structure and energetics of stoichiometric TiO₂ anatase surfaces. *Phys. Rev. B* **2001**, *63*, No. 155409.

- (10) Sanches, F.; Mallia, G.; Liborio, L.; Diebold, U.; Harrison, N. *Phys. Rev. B* **2014**, *89*, No. 245309.

- (11) Wang, Z.-T.; Wang, Y.-G.; Mu, R.; Yoon, Y.; Dahal, A.; Schenter, G. K.; Glezakou, V.-A.; Rousseau, R.; Lyubinetzky, I.; Dohnalek, Z. Probing equilibrium of molecular and deprotonated water on TiO₂ (110). *Proc. Natl. Acad. Sci. U.S.A.* **2017**, *114*, 1801–1805.

- (12) Herman, G.; Dohnalek, Z.; Ruzycki, N.; Diebold, U. Experimental investigation of the interaction of water and methanol with anatase TiO₂ (101). *J. Phys. Chem. B* **2003**, *107*, 2788–2795.

- (13) He, Y.; Tilocca, A.; Dulub, O.; Selloni, A.; Diebold, U. Local ordering and electronic signatures of submonolayer water on anatase TiO₂ (101). *Nat. Mater.* **2009**, *8*, 585–589.

- (14) Vittadini, A.; Selloni, A.; Rotzinger, F. P.; Graetzel, M. Structure and Energetics of Water Adsorbed at TiO₂ anatase(101) and (001) Surfaces. *Phys. Rev. Lett.* **1998**, *81*, 2954–2957.

- (15) Zhao, Z.; Li, Z.; Zou, Z. Understanding the interaction of water with anatase TiO₂ (101) surface from density functional theory calculations. *Phys. Lett. A* **2011**, *375*, 2939–2945.

- (16) Sun, C.; Liu, L.; Selloni, A.; Lu, G. Q.; Smith, S. Titania-water interactions: a review of theoretical studies. *J. Mater. Chem.* **2010**, *20*, 10319–10334.

- (17) Walle, L.; Borg, A.; Johansson, E.; Plogmaker, S.; Rensmo, H.; Uvdal, P.; Sandell, A. Mixed Dissociative and Molecular Water Adsorption on Anatase TiO₂ (101). *J. Phys. Chem. C* **2011**, *115*, 9545–9550.

- (18) Nadeem, I. M.; Treacy, J. P. W.; Selcuk, S.; Torrelles, X.; Hussain, H.; Wilson, A.; Grinter, D. C.; Cabailh, G.; Bikondo, O.; Nicklin, C.; et al. Water Dissociates at the Aqueous Interface with Reduced Anatase TiO₂(101). *J. Phys. Chem. Lett.* **2018**, *9*, 3131–3136.

- (19) Patrick, C. E.; Giustino, F. Structure of a Water Monolayer on the Anatase TiO₂(101) Surface. *Phys. Rev. Appl.* **2014**, *2*, No. 014001.

- (20) Deák, P.; Kullgren, J.; Aradia, B.; Frauenheima, T.; Kavanc, L. Water splitting and the band edge positions of TiO₂. *Electrochim. Acta* **2016**, *199*, 27–34.

- (21) Raju, M.; Kim, S.-Y.; van Duin, A. C. T.; Fichthorn, K. A. ReaxFF Reactive Force Field Study of the Dissociation of Water on Titania Surfaces. *J. Phys. Chem. C* **2013**, *117*, 10558–10572.

- (22) Lindan, P.; Harrison, N.; Holender, J.; Gillan, M. First-principles molecular dynamics simulation of water dissociation on TiO₂(110). *Chem. Phys. Lett.* **1996**, *261*, 246–252.

- (23) Lindan, P. J. D.; Harrison, N. M.; Gillan, M. J. Mixed Dissociative and Molecular Adsorption of Water on the Rutile (110) Surface. *Phys. Rev. Lett.* **1998**, *80*, 762–765.

- (24) Ceriotti, M.; Cuny, J.; Parrinello, M.; Manolopoulos, D. E. Nuclear quantum effects and hydrogen bond fluctuations in water. *Proc. Natl. Acad. Sci. U.S.A.* **2013**, *110*, 15591–15596.

- (25) Li, X.-Z.; Walker, B.; Michaelides, A. Quantum nature of the hydrogen bond. *Proc. Natl. Acad. Sci. U.S.A.* **2011**, *108*, 6369–6373.

- (26) Krukau, A. V.; Vydrov, O. A.; Izmaylov, A. F.; Scuseria, G. E. Influence of the exchange screening parameter on the performance of screened hybrid functionals. *J. Chem. Phys.* **2006**, *125*, No. 224106.

(27) Janesko, B. G.; Henderson, T. M.; Scuseria, G. E. Screened hybrid density functionals for solid-state chemistry and physics. *Phys. Chem. Chem. Phys.* **2009**, *11*, 443–454.

(28) Pernot, P.; Civalleri, B.; Presti, D.; Savin, A. Prediction Uncertainty of Density Functional Approximations for Properties of Crystals with Cubic Symmetry. *J. Phys. Chem. A* **2015**, *119*, 5288–5304.

(29) Paier, J.; Marsman, M.; Hummer, K.; Kresse, G.; et al. Screened hybrid density functionals applied to solids. *J. Chem. Phys.* **2006**, *124*, No. 154709.

(30) Garza, A. J.; Scuseria, G. Predicting band gaps with hybrid density functionals. *J. Phys. Chem. Lett.* **2016**, *7*, 4165–4170.

(31) Viñes, I.; Lamiel-Garcia, O.; Ko, K. C.; Lee, J. Y.; Illas, F. Systematic Study of the Effect of HSE Functional Internal Parameters on the Electronic Structure and Gap of a Representative Set of Metal Oxides. *J. Comput. Chem.* **2017**, *38*, 781–789.

(32) Dovesi, R.; Orlando, R.; Erba, A.; Zicovich-Wilson, C. M.; Civalleri, B.; Casassa, S.; Maschio, L.; Ferrabone, M.; Pierre, M. D. L.; D'Arco, P.; et al. CRYSTAL14: A program for the ab initio investigation of crystalline solids. *Int. J. Quantum Chem.* **2014**, *114*, 1287–1317.

(33) Monkhorst, H. J.; Pack, J. D. Special points for Brillouin-zone integrations. *Phys. Rev. B* **1976**, *13*, 5188–5192.

(34) Pisani, C.; Dovesi, R.; Roetti, C. *Hartree-Fock ab initio Treatment of Crystalline Systems*; Springer, 1988.

(35) Dahal, A.; Dohnalek, Z. Formation of Metastable Water Chains on Anatase TiO₂(101). *J. Phys. Chem. C* **2017**, *121*, 20413–20418.

(36) Desiraju, G.; Steiner, T. *The weak hydrogen bond in structural chemistry and biology*; Oxford University Press, 1999.

(37) Grimme, S.; Antony, J.; Ehrlich, S.; Krieg, S. A consistent and accurate ab initio parametrization of density functional dispersion correction (dft-d) for the 94 elements H–Pu. *J. Chem. Phys.* **2010**, *132*, No. 154104.

(38) Casado, R. M.; Todorović, M.; Mallia, G.; Harrison, N.; Pérez, R. First principles calculations on defective (101) anatase surface: influence of basis sets and exchange functionals. *J. Phys. Chem. C*, **2017**.

(39) Stetsovych, O.; Todorović, M.; Shimizu, T. K.; Moreno, C.; Ryan, J. W.; León, C. P.; Sagisaka, K.; Palomares, E.; Matolín, V.; Fujita, D.; et al. Atomic species identification at the (101) anatase surface by simultaneous scanning tunnelling and atomic force microscopy. *Nat. Commun.* **2015**, *6*, No. 7265.

(40) Aschauer, U.; He, Y.; Cheng, H.; Li, S.-C.; Diebold, U.; Selloni, A. Influence of Subsurface Defects on the Surface Reactivity of TiO₂: Water on anatase(101). *J. Phys. Chem. C* **2010**, *114*, 1278–1284.

(41) Patel, M.; Sanches, F.; Mallia, G.; Harrison, N. A quantum mechanical study of water adsorption on the (110) surfaces of rutile SnO₂ and TiO₂: investigating the effects of intermolecular interactions using hybrid-exchange density functional theory. *Phys. Chem. Chem. Phys.* **2014**, *16*, 21002–21015.